Mechanistic study of the hydrolysis of nitrocefin mediated by *B.cereus* metallo-β-lactamase

Rodolfo M. Rasia and Alejandro J. Vila*

Area Biofísica and Instituto de Biología Molecular y Celular de Rosario (IBR)
Facultad de Ciencias Bioquímicas y Farmacéuticas, Universidad Nacional de Rosario
Suipacha 531, Rosario 2000, Argentina
E-mail: vila@arnet.com.ar / avila@fbioyf.unr.edu.ar

Dedicated to Professor Edmundo A.Rúveda on his 70th birthday and to Professor Roberto Rossi on his 60th birthday

(received 28 Jul 03; accepted 22 Oct 03; published on the web 30 Nov 03)

Abstract

The hydrolysis of the β-lactam compound nitrocefin by the metallo-β-lactamase from *B.cereus* (BcII) was studied by pre-steady state kinetics measurements, followed by absorbance, fluorescence and diode array detection. In contrast with the results reported for the homologous enzymes CcrA from *B.fragilis* and L1 from *S.maltophilia*, no accumulation of an anionic intermediate could be evidenced. The rationale for this observation can be tracked on the lower binding affinity toward a second Zn(II) ion in this enzyme, and the modification of a flexible active site loop, that might contribute to stabilize the anionic intermediate. Analysis of the substrate binding and product formation rates does not support a recently proposed mechanistic scheme that contemplates a non-negligible accumulation of this intermediate in nitrocefin hydrolysis by BcII.

Keywords: Metallo-β-lactamases, Zinc enzymes, pre-steady-state kinetics

Introduction

Bacterial resistance to β-lactam antibiotics is mostly due to the production of β-lactamases [1]. These enzymes are able to inactivate the β-lactam antibiotics by hydrolyzing the four-membered β-lactam ring. Among this family of enzymes, metallo-β-lactamases constitute a distinct class in several aspects [2-4]. These metalloenzymes are well known for exhibiting a broad substrate spectrum, being able to hydrolyze most of the β-lactam antibiotics currently available. The spread of metallo-β-lactamase genes among pathogenic bacterial strains is raising an increasing concern in the biomedical community, as no clinically useful inhibitors have been developed yet[5].

The successful development of appropriate inhibitors largely relies on the elucidation of the mechanism of the reaction catalyzed by the title enzyme. The hydrolysis of β-lactams by metallo-β-

lactamases proceeds through an initial nucleophilic attack to the carbonyl carbon of the substrate by a Zn-bound hydroxide moiety, leading to the formation of a tetrahedral species [4] (Figure 1). Pre steady state kinetic studies on the metallo-β-lactamases from *Bacteroides fragilis* (CcrA) [6] and from *Stenotrophomonas maltophilia* (L1) [7] have shown that the hydrolysis of the cromophoric cephalosporin nitrocefin proceeds through an anionic intermediate, that can be identified spectroscopically. This intermediate is formed after the nucleophilic attack on the substrate by cleavage of the C-N bond, which leaves the N atom negatively charged. The final (and rate limiting) step in the reaction is the protonation of the N atom, after which the product is released [8]. Formation of this intermediate is due to the particular chemical nature of nitrocefin, which allows the stabilization of the negative charge in the π system of its dinitrostyryl substituent. This makes nitrocefin an excellent substrate to probe the catalytic mechanism of these enzymes.

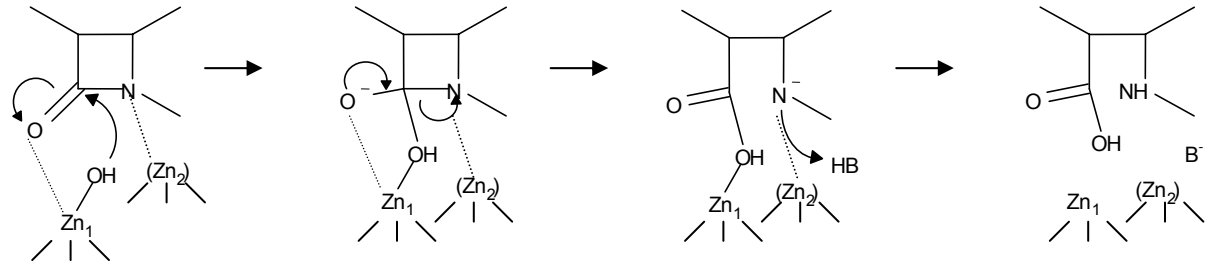

Figure 1. Reaction mechanism of metallo-β-lactamases.

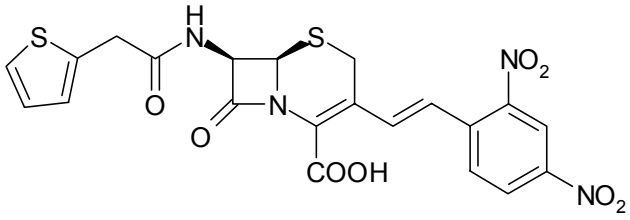

Figure 2. Structure of nitrocefin.

The metallo-β-lactamase from *B.cereus* (BcII) displays several differences with the enzymes CcrA and L1. While the latter enzymes are isolated with two zinc ions bound per enzyme, both of which seem to be essential for the mechanism, BcII binds two equivalents of Zn(II), but with quite different affinities [9-11]. The active species *in vivo* for BcII is purportedly the mono-Zn(II) derivative, even if the bi-Zn(II) form shows a higher catalytic efficiency. With the aim of generating a more complete picture of the mechanistic aspects of β-lactam hydrolysis by metallo-β-lactamases, we studied the pre-steady state kinetics of the reaction of BcII with nitrocefin.

Results and Discussion

Kinetic measurement of substrate binding

As already reported for the enzyme L1 from *S. maltophilia*, nitrocefin binding to BcII results in quenching of the enzyme intrinsic fluorescence [12]. This process can be studied independently of the hydrolytic reaction. Thus, the analysis of this event under pseudo first order conditions may yield the individual rate constants for nitrocefin binding to BcII. The kinetic traces obtained at different nitrocefin concentrations are shown in Figure 3A. The slight curvature of this plot suggests a two-step binding process (see Scheme 1). The data points were then fitted to the following hyperbolic function:

$$k_{obs} = k_{cat} + k_{-2} + k_{+1} \cdot [\text{nitrocefin}] / (K_1 + [\text{nitrocefin}]) \quad (1)$$

where K_1 is the pre-equilibrium dissociation constant, k_{+2} and k_{-2} are the forward and reverse constants of the second step, and k_{cat} is the rate constant for conversion of substrate to product (Scheme 1, Figure 3A). Although neither k_{+2} nor k_{-2} is well defined by the experimental data, a linear fit of the rate constants resulted in biased residual plots, and therefore we decided to include the two binding steps in the reaction scheme. Due to the low substrate concentrations used (relative to the dissociation constant K_1), the estimates of the individual values of K_1 and k_{+2} are not well defined, but rather the pseudo second order rate constant for the formation of $E{\cdot}S_2$, $k_{+2}/K1$ is accurately estimated. The low value obtained for $k_{-2} + k_{cat}$ and its high standard deviation indicate that the second step is essentially irreversible. To obtain a more precise estimation of the rate constants, simultaneous fit of all datasets was performed using the software DynaFit[13]; the initial parameters used were those obtained from the hyperbolic fit of the individual rate constants (Table 1).

$$E + S \underset{k_{-1}\ (K_1)}{\overset{k_{+1}}{\leftrightarrow}} E{\cdot}S_1 \overset{K_{+2}}{\underset{k_{-2}}{\leftrightarrow}} E{\cdot}S_2 \xrightarrow{k_{cat}} E + P$$

Scheme 1. Proposed mechanistic scheme for the reaction of BcII with nitrocefin. In both enzyme-substrate complexes ($E{\cdot}S_1$, $E{\cdot}S_2$) the substrate is bound to the enzyme, but has not undergone any chemical modification. All bond formation and breaking steps occur in a concerted way with a rate equal to k_{cat}.

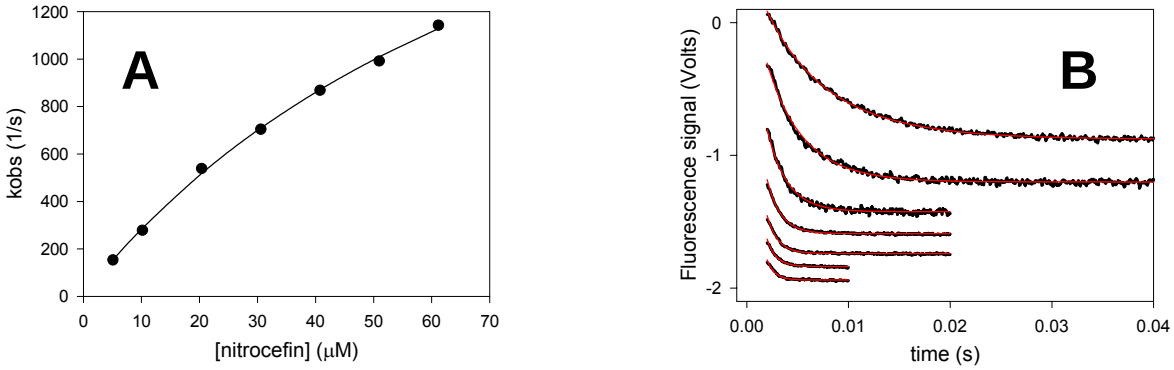

Figure 3. Pseudo first order data analysis. **(A).** Plot of the pseudo first order rate constants obtained from individual exponential fits of the reaction traces performed at different nitrocefin concentrations. The line corresponds to the hyperbolic fit (Eq 1.). **(B).** Global fit of the pseudo first order data. The black thick lines correspond to the reaction of 1 μM BcII with 5, 10, 20, 31, 41, 51 and 61 μM nitrocefin. The offset of the traces is due to inner filter effects at increasing nitrocefin concentration. Red lines correspond to the global fit.

Table 1. Kinetic rate constants

	Estimated from hyperbolic fit	Global fit pseudo first order	Global fit hydrolysis
k_{+1}	89 ± 16 μM [a]	10^8 $M^{-1}·s^{-1}$ (fixed)	10^8 $M^{-1}·s^{-1}$ (fixed)
k_{-1}		11000 ± 280 s^{-1}	11000 s^{-1} (fixed)
k_{+2}	2760 ± 280 s^{-1}	4400 ± 90 s^{-1}	4400 s^{-1} (fixed)
k_{-2}	4 ± 23 s^{-1} [b]	55.6 ± 0.3s^{-1}	55.6 s^{-1} (fixed)
k_{cat}			4.70 ± 0.01 s^{-1}

[a] Corresponds to K_1 (k_{-1}/k_{+1}).

[b] Corresponds to $k_{-2} + k_{cat}$.

Kinetic measurement of the hydrolytic reaction

The hydrolysis of nitrocefin and the formation of product can be followed through monitoring the absorbance at 390 and 485 nm respectively. Nitrocefin hydrolysis by BcII was studied under single turnover conditions using the photodiode array to determine whether an intermediate species similar to that seen with CcrA or L1 was formed during the reaction. The rates of substrate depletion and product formation were similar ($k_{substrate}$ = 4.5 s^{-1}; $k_{product}$ = 4.4 s^{-1}), and no spectral feature was apparent at > 600 nm (Figure 4). This can be interpreted by assuming that the reaction proceeds through a reaction intermediate different from that reported for L1 and CcrA, or that, if formed, its concentration is below the detection limit.

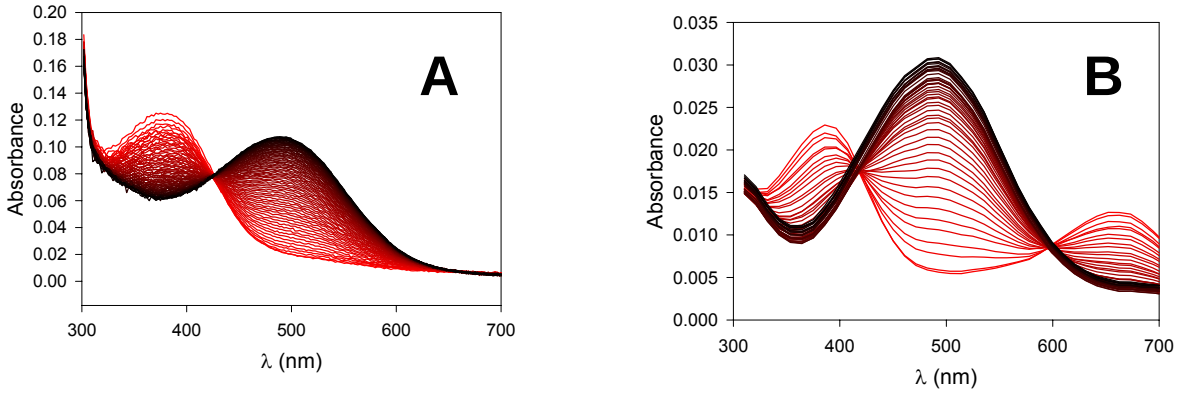

Figure 4. Reaction of BcII (A) and CcrA (B) with nitrocefin measured using a photodiode array detector. 400 spectra were collected with 1.25 ms integration time for a total acquisition time of 0.5 s. Spectra are colored using a gradient from red (first spectrum) to black (last spectrum). **(A).** 22.5 μM BcII vs. 6.3 μM nitrocefin, 15ºC. One out of five spectra is shown for clarity. No spectral feature is apparent over 600 nm. **(B).** 5 μM CcrA vs. 14 μM nitrocefin, 25ºC. All spectra are shown until 65 ms (reaction completion time).

A fast initial decay in absorbance at 390 nm (substrate) was apparent from a close inspection of the reaction traces shown in Figure 4, but the time resolution of the photodiode array was not sufficient to neatly resolve a different process. The study of the same reaction by following the absorbance at a fixed wavelength using a photomultiplier tube allowed us to resolve a double exponential decay at 390 nm (Figure 5). The reaction was also followed by absorption at 485 nm (product), and through the variation of the protein intrinsic fluorescence (substrate binding and product release). To exclude the possibility that the initial decay at 390 nm could be an artifact, the reaction was monitored by using two different enzyme concentrations and two different substrate concentrations. A global fit of these reaction curves, using the binding rate constants obtained previously, yielded a value for k_{cat} (Table 1). The initial part of the traces (0.1 s) was fitted to the following function:

$$\text{Abs} = a_{390} \cdot \exp(-k^0_{390} * t) - v*t \qquad (2)$$

where a_{390} and k^0_{390} are the amplitude and the rate constant of the initial exponential process respectively, and v is the initial rate of the second exponential process. Both the amplitude and the rate constant of the initial exponential process increased with increasing substrate and/or enzyme concentration (Table 2). The values of these rate constants (k^0_{390}) were similar to those describing the quenching of the intrinsic enzyme fluorescence. These results suggest that formation of the quenched $E{\cdot}S_2$ complex gives rise to an alteration of the substrate spectrum, with a reduced absorptivity at 390 nm. In order to demonstrate that the data obtained are consistent with a change in absorptivity, the absorbance traces were subject to a global fit with DynaFit, using the reaction scheme and rate constants previously determined. The resulting fit satisfactorily matches the experimental traces, yielding an ε_{390} value of 15000 $M^{-1}{\cdot}cm^{-1}$ for the $E{\cdot}S_2$ complex, compared to an

ε_{390} of 17000 $M^{-1}\cdot cm^{-1}$ for free nitrocefin (which is assumed to be identical to that of the $E\cdot S_1$ complex) (Figure 5A).

Table 2. Analysis of the initial burst observed in the absorbance at 390 nm traces

[BcII]	[Nitrocefin]	K^0_{390}	a_{390}	$k_{fluor.}$
10 μM	3.8 μM	192 ± 7 s^{-1}	0.8 ± 0.01 mAU	196 ± 1 s^{-1}
	7.2 μM	236 ± 6 s^{-1}	1.3 ± 0.01 mAU	218 ± 2 s^{-1}
30 μM	12 μM	304 ± 5 s^{-1}	3.1 ± 0.01 mAU	360 ± 2 s^{-1}
	23 μM	348 ± 5 s^{-1}	3.5 ± 0.01 mAU	363 ± 3 s^{-1}

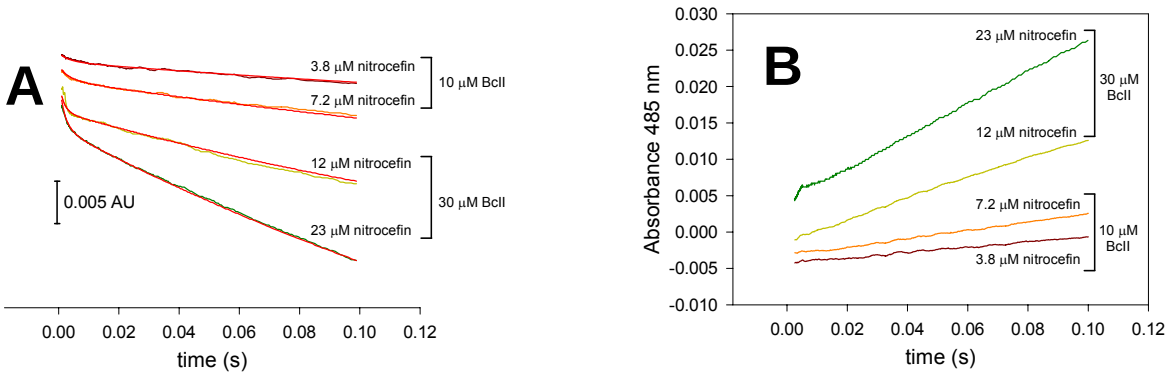

Figure 5. Initial portion of the absorbance at 390 and 485 nm traces. **(A).** Reaction traces of absorbance at 390 nm. The traces were offset to improve visualization, as the initial absorbance values vary greatly. The absorbance scale is indicated by the bar on the left. The red lines correspond to the global fit of the data. **(B).** Reaction traces of absorbance at 485 nm.

A decrease in absorptivity can be explained by a shift in the absorption maximum of the substrate bound to the enzyme. A close analysis of the absorbance traces at 485 nm (product formation) shows an initial burst, with a very low amplitude (Figure 4B). Put together, these results are consistent with a red shift of the substrate spectrum upon binding to the enzyme. An intermediate in nitrocefin hydrolysis by BcII with a red shifted absorption maximum was already reported by Bicknell and Waley in cryosolvents at sub zero temperatures [14], who also reported that spectral shifts of this kind occur to nitrocefin when lowering the solvent polarity.

Subclass B1 metallo-β-lactamases have a flexible loop which closes upon substrate binding [15-17]. This loop was shown to contribute to create a hydrophobic pocket in the active site cavity upon substrate binding, which would give rise in the case of nitrocefin to the red shift of the absorption maximum.

In summary, the information gathered with the single turnover experiments points to the existence of only one significantly populated intermediate, in which the substrate has not undergone any chemical reaction, and is buried in the enzyme active site displaying a red shift of its absorption spectrum.

Comparison with another mechanistic model proposed

In a recent paper [17], the accumulation of an anionic intermediate during the hydrolysis of nitrocefin catalyzed by BcII was suggested. Based on the results obtained from absorbance data at 390, 485 and 660 nm, the authors proposed a linear kinetic mechanism (Scheme 2) similar to the one shown here, but with striking differences in the absolute values of the individual rate constants and in the identity of the intermediate species formed. In the work by Moali and coworkers, values of the individual rate constants were calculated to agree with the experimental rates of substrate consumption, product formation and the steady state kinetic parameters. Instead, the rate constants presented in this work were obtained from direct observation of all the proposed reaction intermediates.

$$\mathrm{E + S} \underset{k_{-1}\ 1100\ s^{-1}}{\overset{k_{+1}\ 10^8\ M^{-1}\cdot s^{-1}}{\leftrightarrow}} \mathrm{E\cdot S} \xrightarrow[23\ s^{-1}]{k_2} \mathrm{E\cdot I} \xrightarrow[920\ s^{-1}]{k_3} \mathrm{E\cdot P} \xrightarrow[>1000\ s^{-1}]{k_4} \mathrm{E + P}$$

Scheme 2. Reaction of BcII with nitrocefin [17]. In the E·S complex, the substrate is still intact. E·I corresponds to the anionic intermediate that appears in the reaction of CcrA and L1 with nitrocefin (Figure 1). In E·P, the product is already formed but still bound to the enzyme. Both k_2 and k_3 are chemical steps (cleavage of the lactam bond and protonation of the intermediate respectively).

A simulation of the reaction time course with the software DynaFit using Scheme 2 shows that the more populated reaction intermediate is E·S, but it reaches its maximal concentration at *ca.* 0.6 ms, which is well below the dead time of our measurements. The fluorescence quenching observed by us (*ca.* 40%) reveals the existence of a highly populated reaction intermediate. However, the simulation indicates that neither E·I, nor E·P reaches a concentration high enough to account for the observed quenching.

Despite the mentioned differences between the two models, we cannot discard the formation of the proposed anionic intermediate. In our hands, no evidences for the accumulation of such an intermediate could be obtained. In fact, hydrolyzed nitrocefin absorbs at 660 nm with an extintion coefficient of 400 $M^{-1}\cdot cm^{-1}$. In the conditions tested in this work, the absorbance at 660 nm increases steadily during the reaction with the same rate displayed by absorbance at 485 nm, *i.e.* concomitant with product formation. If the anionic intermediate were formed to an amount greater than 1% of the total product present in the reaction, its consumption to form product would be noticeable as a decrease in absorbance at 660 nm. This would be particularly evident under single turnover conditions, in which the concentration of reaction intermediates relative to substrate and product is the highest. Hence, our experimental data indicate that the anionic intermediate (if present) does not accumulate to more than 1% of the total product concentration during the reaction.

This fact reveals that, in contrast with the enzymes CcrA and L1, BcII does not favor cleavage of the β-lactam bond without protonation of the leaving amide.

Conclusions

The inability to detect the accumulation of the anionic intermediate during nitrocefin hydrolysis by BcII lead us to conclude that BcII lacks some structural features present in the metallo-β-lactamases CcrA and L1, that contribute to stabilize this intermediate. These features are:

1. The presence of a tightly formed binuclear metal binding site, in which Zn_2 acts as a superacid to stabilize the negative charge developed at the β-lactam nitrogen [18]. In contrast with CcrA and L1, the Zn_2 site in BcII seems to be not fully occupied and Zn_2 is more loosely bound.
2. The length and aminoacid composition of the active site flexible loop. It was shown that transplantation of a different loop into BcII results in a significant increase in the accumulation of the anionic intermediate [17]. In L1, several other loops are present around the active site.

Although the results obtained with nitrocefin cannot be directly extrapolated to the reaction of metallo-β-lactamases with other substrates, they show that lactamases from pathogenic bacteria have evolved to improve catalysis by stabilization of a transition state different from that present in the relatively innocuous *B.cereus* strains. The selective pressure imposed by antibiotics misuse can clearly lead to the improvement of metallo-β-lactamase reactivity.

Experimental Section

Reagents. All chemicals were of the best quality available. Nitrocefin was a kind gift from Glaxo Welcome. 20 mM stock solutions of nitrocefin were prepared dissolving the solid compound in DMSO. The concentration of the stock solution was determined spectrophotometrically, measuring the ΔAbs at 485 nm after complete hydrolysis ($\Delta\varepsilon_{485}$ = 17400 $M^{-1}\cdot cm^{-1}$).

Enzyme samples. Expression and purification of BcII was performed as previously reported. Purity of the enzyme preparations was checked by SDS-PAGE. Protein samples used in all experiments reported were exchanged from the final purification buffer to Hepes 15 mM pH 7.5 using a HiPrep® 26/10 desalting column (Amersham Pharmacia Biotech) or by two dialysis steps against >100 volumes of the same buffer. The Zn(II) content was measured using the colorimetric reagent 4-(2-pyridylazo)-resorcinol (PAR) [19].

Pre steady state kinetic data obtention and analysis. Experiments were carried on an Applied Photophysics SX.18-MVR stopped flow spectrometer. Enzyme fluorescence measurements were performed exciting at 280 nm (slit width = 0.5 mm) and detecting through a cutoff filter at >305 nm. The photomultiplier voltage was set to obtain a 4.0 V or 0.8 V signal with the free enzyme. The background signal obtained after washing the observation cell with buffer ranged within 0.1-0.2 V. Absorbance changes were measured at the corresponding λ_{max} for substrate or product using an absorption photomultiplier. The reference was set with buffer in the observation cell. For both

absorbance and fluorescence measurements the excitation/absorption pathlength was 0.2 cm. Reactions with nitrocefin were also followed in the 300-700 nm range using the PD.1 photodiode array detector. All reactions were performed in Hepes 15 mM, pH 7.5 without extra Zn(II) added. The whole sample head was kept at 15 ºC using a Lauda RC6 thermostatted circulator.

Pseudo first order data on substrate binding were obtained mixing 2 μM enzyme solutions with 10 to 160 μM substrate (syringe concentration), and measuring the protein intrinsic fluorescence on a split timebase. Typically, 5-10 runs were averaged when k_{obs} exceeded 500 s^{-1} to improve the signal-to-noise ratio. Quenching of the enzyme fluorescence was satisfactorily fitted to simple exponential functions, yielding standard deviations below 1%. The dependence of the observed rate constants with substrate concentrations were subject to a nonlinear fit to yield K_1, k_{+2}, and $k_{-2} + k_{cat}$. Nonlinear fits of the experimental data were performed using the software Sigma Plot; the reported standard deviations are those informed by the nonlinear fitting algorithm. The initial portions of the curves were subject to global fit using the software DynaFit, yielding the reported values for k_{-1}, k_{+2} and k_{-2}. The standard deviations indicated by the program are reported.

Single turnover experiments were performed at enzyme concentrations of 20 or 60 μM and substrate concentrations of 7.6, 14.4, 24 and 46 μM. Substrate consumption, product formation and enzyme fluorescence were recorded.

Steady state kinetic parameters in the same conditions used for the pre-steady state experiments were obtained by recording the whole reaction time courses of substrate consumption, and fitting to the integrated form of the Michaelis-Menten equation.

Acknowledgments

RMR is recipient of a doctoral fellowship from CONICET. AJV is a Staff member from CONICET and an International Research Scholar of the Howard Hughes Medical Institute. This work has been supported by grants from CONICET (PIP 98), ANPCyT and HHMI. We thank Drs. Walt Fast and Stephen J. Benkovic for providing us with the expression plasmid for the *B.fragilis* metallo-β-lactamase CcrA. RMR thanks the instructors and participants of the 2002 EMBO workshop on transient kinetics applied to biological macromolecules.

References

1. Frère, J. M. *Molecular Microbiology* **1995**, *16*, 385.
2. Cricco, J. A.; Rasia, R. M.; Orellano, E. G.; Ceccarelli, E. A.; Vila, A. J. *Coord. Chem. Rev.* **1999**, *190-192*, 519.
3. Cricco, J. A. and Vila, A. J. *Curr. Pharm. Des.* **1999**, *5*, 915.
4. Wang, Z.; Fast, W.; Valentine, A. M.; Benkovic, S. J. *Curr. Opin. Chem Biol.* **1999**, *3*, 614.
5. Matagne, A.; Dubus, A.; Galleni, M.; Frere, J. M. *Nat. Prod. Rep.* **1999**, *16*, 1.
6. Wang, Z.; Fast, W.; Benkovic, S. J. *J. Am. Chem. Soc.* **1998**, *120*, 10788.

7. McManus-Muñoz, S. and Crowder, M. W. *Biochemistry* **1999**, *38*, 1547.
8. Wang, Z.; Fast, W.; Benkovic, S. J. *Biochemistry* **1999**, *38*, 10013.
9. Orellano, E. G.; Girardini, J. E.; Cricco, J. A.; Ceccarelli, E. A.; Vila, A. J. *Biochemistry* **1998**, *37*, 10173.
10. Paul-Soto, R.; Bauer, R.; Frère, J. M.; Galleni, M.; Meyer-Klaucke, W.; Nolting, H.; Rossolini, G. M.; de Seny, D.; Hernández Valladares, M.; Zeppezauer, M.; Adolph, H. W. *J. Biol. Chem.* **1999**, *274*, 13242.
11. Rasia, R. M. and Vila, A. J. *Biochemistry* **2002**, *41*, 1853.
12. Spencer, J.; Clarke, A. R.; Walsh, T. R. *J. Biol. Chem.* **2001**, *276*, 33638.
13. Kuzmic, P. *Anal. Biochem.* **1996**, *237*, 260.
14. Bicknell, R. and Waley, S. G. *Biochemistry* **1985**, *24*, 6876.
15. Huntley, J. J.; Scrofani, S. D.; Osborne, M. J.; Wright, P. E.; Dyson, H. J. *Biochemistry* **2000** , *39*, 13356.
16. Toney, J. H.; Fitzgerald, P. M. D.; Grover-Sharma, N.; Olson, S. H.; May, W. J.; Sundelof, J. G.; Vanderwall, D. E.; Cleary, K. A.; Grant, S. K.; Wu, J. K.; Kozarich, J. W.; Pompliano, D. L.; Hammond, G. G. *Chemistry & Biology* **1998**, *5*, 185.
17. Moali, C.; Anne, C.; Lamotte-Brasseur, J.; Groslambert, S.; Devreese, B.; van Beeumen, J.; Galleni, M.; Frere, J. M. *Chemistry & Biology* **2003**, *10*, 319.
18. Fast, W.; Wang, Z.; Benkovic, S. J. *Biochemistry* **2001**, *40*, 1640.
19. McCall, K. A.; Fierke, C. A. *Anal. Biochem.* **2000**, *284*, 307.